Acta Cryst E CRYSTALLOGRAPHIC COMMUNICATIONS

ISSN 2056-9890

Crystal structure of a new polymorph of 3-acetyl-8-methoxy-2*H*-chromen-2-one

Gabino Gonzalez-Carrillo,[a] Roberto Muñiz-Valencia,[a] Efren V. García-Báez[b] and Francisco J. Martínez-Martínez[a]*

[a]Facultad de Ciencias Químicas, Universidad de Colima, km 9 carretera, Colima-Coquimatlán, 28400, Coquimatlán, Colima, Mexico, and [b]Laboratorio de Quimica Supramolecular y Nanociencias, Unidad Profesional, Interdisciplinaria de Biotecnología, Instituto Politécnico Nacional, Avenida Acueducto s/n, Barrio La Laguna Ticomán, Cd. de Mexico 07340, Mexico. *Correspondence e-mail: fjmartin@ucol.mx

Received 2 September 2019
Accepted 9 November 2019

Edited by D. Chopra, Indian Institute of Science Education and Research Bhopal, India

Keywords: crystal structure; polymorph; hydrogen bond; coumarin; 3-acetyl-8-methoxy-coumarin.

CCDC reference: 1964910

Supporting information: this article has supporting information at journals.iucr.org/e

A new polymorphic form of the title compound, $C_{12}H_{10}O_4$, is described in the orthorhombic space group *Pbca* and $Z = 8$, as compared to polymorph I, which crystallizes in the monoclinic space group *C*2/*c* and $Z = 8$ [Li *et al.* (2012). *Chin. J. Struct. Chem.* **31**, 1003–1007.]. In polymorph II, the coumarin ring system is almost planar (r.m.s. deviation = 0.00129 Å). In the crystal, molecules are connected by Csp^3—H···O and C_{ar}—H···O hydrogen bonds, forming molecular sheets linked into zigzag shaped layers along the *b*-axis direction. The three-dimensional lattice is assembled through stacking of the zigzag layers by π–π interactions with a centroid-to-centroid distance of 3.600 (9) Å and antiparallel C=O···C=O interactions with a distance of 3.1986 (17) Å, which give rise to a helical supramolecular architecture.

1. Chemical context

Derivatives of 2*H*-chromen-2-one are some of the most important heterocycles in natural and synthetic organic chemistry. These substances are bioactive compounds and have a wide range of applications in the medical field (Gaudino *et al.*, 2016) showing, for example, anti-HIV, anti-mutagenic, anticancer and antitumor activities among others (Vekariya & Patel, 2014). They are synthesized using classical methodologies such as the Pechmann or Knoevenagel reactions, as well as recent methodologies such as the metathesis cyclization (Salem *et al.*, 2018) or alkynoates cyclization (Liu *et al.*, 2018).

The disposition of the crystalline lattices of coumarin derivatives is driven by a great variety of intermolecular interactions (Santos-Contreras *et al.*, 2009). This working group has reported the participation of π–π stacking interactions, hydrogen-bonding and dipole–dipole interactions involving the carbonyl group (Gómez-Castro *et al.*, 2014) in the determination of the 1D, 2D and 3D supramolecular assemblies of crystalline structures for different compounds (González-Padilla *et al.*, 2014). This report describes the structure of a second polymorph of the title compound and the importance of C—H···O, C=O···C=O and π–π stacking intermolecular interactions in crystal packing.

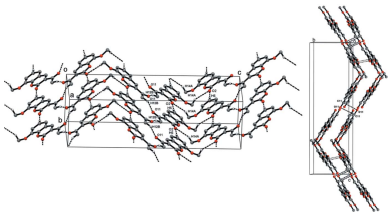

2. Structural commentary

The title polymorph II (Fig. 1) crystallizes in the orthorhombic system, space group *Pbca*, with eight molecules in the unit cell

whereas polymorph I (Li *et al.*, 2012) crystallizes in the monoclinic system in space group *C*2/*c*, also with eight molecules in the unit cell. In polymorph II, the coumarin skeleton is almost planar (r.m.s. deviation = 0.00129 Å) with dihedral angles O1—C9—C10—C5 and C8—C9—C10—C4 of 179.20 (10) and 179.87 (11)°, respectively. In contrast, in polymorph I the benzene and lactone rings deviate slightly from planarity by 2.76 (3)°. The acetyl and methoxy groups of polymorph II are almost coplanar with the coumarin ring, with torsion angles C2—C3—C11—C12 = −1.25 (18)° and C14—O13—C8—C7 = −2.70 (18)°.

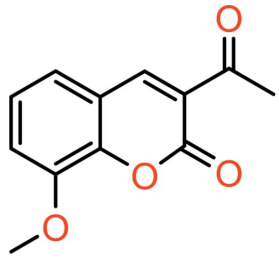

3. Supramolecular features

The crystal network of the title compound (polymorph II) is assembled by zigzag shaped molecular layers that extend approximately in the (012) and (01$\bar{2}$) planes, forming an angle of 116.2°. In the flat section of the zigzag layer $R_3^3(18)$ motifs are formed by C6—H6···O2^{ii} and C12—H12*B*···O11^{i} hydrogen bonds (Table 1). These intermolecular interactions impart stability to the 2D sheet, while weak C14—H14*A*···O2^{iii} interactions generate an $R_3^2(16)$ motif at the intersection of the planes (Fig. 2). Adjacent layers, separated by a distance of 3.4083 (5) Å, are connected by π–π stacking interactions with a centroid-to-centroid distance of 3.600 (9) Å and a slippage of 1.160 Å. In addition to the π stacking, layers are stabilized by antiparallel C═O···C═O interactions (Allen *et al.*, 1998) involving the acetyl group separated by a distance of 3.1986 (17) Å.

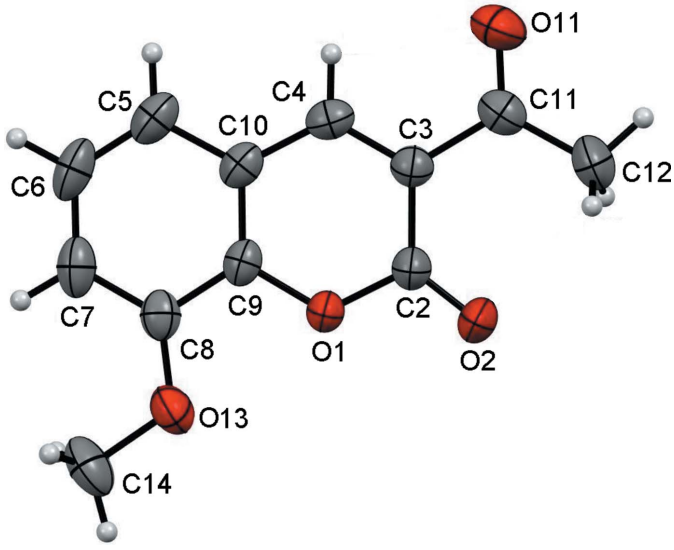

Figure 1
ORTEP plot of polymorph II of the title compound with the atom-numbering scheme. Displacement ellipsoids are drawn at the 50% probability level.

Table 1
Hydrogen-bond geometry (Å, °).

D—H···*A*	*D*—H	H···*A*	*D*···*A*	*D*—H···*A*
C12—H12*B*···O11^{i}	0.96	2.63	3.4255 (17)	141
C6—H6···O2^{ii}	0.93	2.45	3.3808 (16)	176
C14—H14*A*···O2^{iii}	0.96	2.68	3.4535 (18)	138

Symmetry codes: (i) $x+\frac{1}{2}, -y+\frac{3}{2}, -z+1$; (ii) $x-1, y, z$; (iii) $x-\frac{1}{2}, y, -z+\frac{1}{2}$.

The supramolecular array of polymorph II exhibits a helical conformation, like polymorph I (Li *et al.*, 2012). However, in polymorph II the C═O···C═O interactions form the central axis of the helix whilst π–π interactions between the aromatic and lactone rings, aligned in a head-to-tail conformation, control the rotation of the structure. In polymorph I, the helical axis is built by hydrogen bonds and face-to-face π–π stacking interactions of the benzofused rings (Fig. 3). For polymorph I, a complete rotation of the helix is performed in 11.5 Å, while in polymorph II the displacement of the helix in a whole rotation is 12.4 Å.

4. Hirshfeld surface and 2D fingerprint plots

In order to better understand the crystal packing of both polymorphs, Hirshfeld surface analyses and 2D fingerprint plots were carried out using *Crystal Explorer 17.5* (Turner *et al.*, 2017). From the analysis of the Hirshfeld surfaces (Fig. 4), it is evident that there are differences between the chemical environments of these two identical molecules. In Fig. 4, the Hirshfeld surfaces for polymorph I show a series of strong short contacts (big red dots) corresponding to hydrogen bonds stabilizing the 2D sheets. The planar areas above and below the rings are where π–π interactions (small red dots) take place, giving rise to the 3D network. On the other hand, polymorph II is stabilized by a short directional hydrogen bond and the sum of weak interactions with longer contact distances than in polymorph I. This suggests that polymorph II may be the less stable between these two phases of the title compound. To quantitatively compare polymorphs I and II in terms of their crystal packing, 2D fingerprint plots were developed and analysed. The character of the fingerprints plots for both polymorphs is similar, with small differences in the relative contributions of each type of interaction to the Hirshfeld surface. The weak interactions include C···H (C—H···π), C···O (C═O···C═O, C═O···π) and C···C (π–π), as well as short directional interactions such as H···O (Fig. 5).

Although polymorphs I and II exhibit the same type of intermolecular interactions, the way these common interactions contribute to the packing in each polymorph differs in each case. The minor differences in which weak intermolecular interactions contribute to the formation of the crystal (Fig. 6), give rise to distinct polymorphs as suggested by Hasija & Chopra (2019). As can be seen in Fig. 6, the major

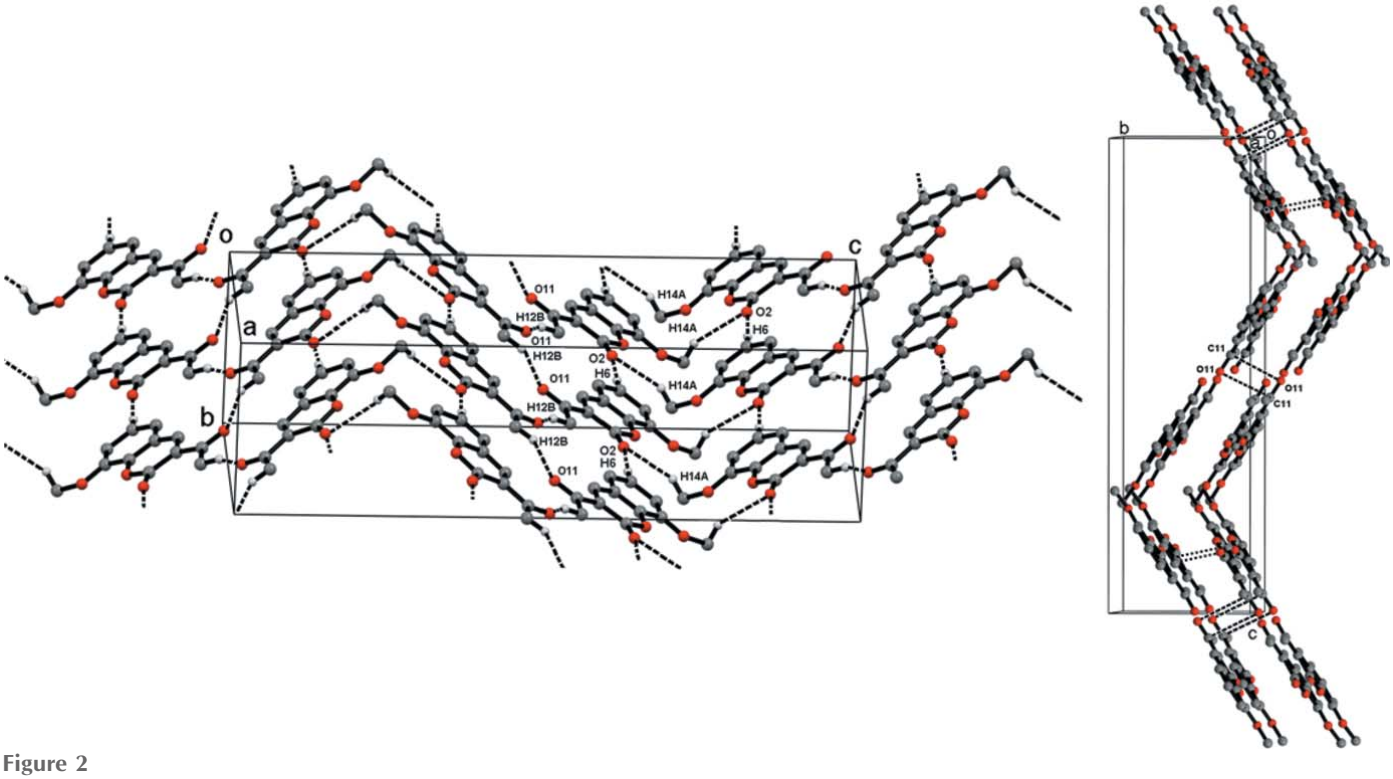

Figure 2
Packing of molecules in polymorph II by C—H···O hydrogen bonding and the packing of parallel sheets connected *via* C═O···C═O and weak π–π interactions. Dotted lines depict the intermolecular interactions.

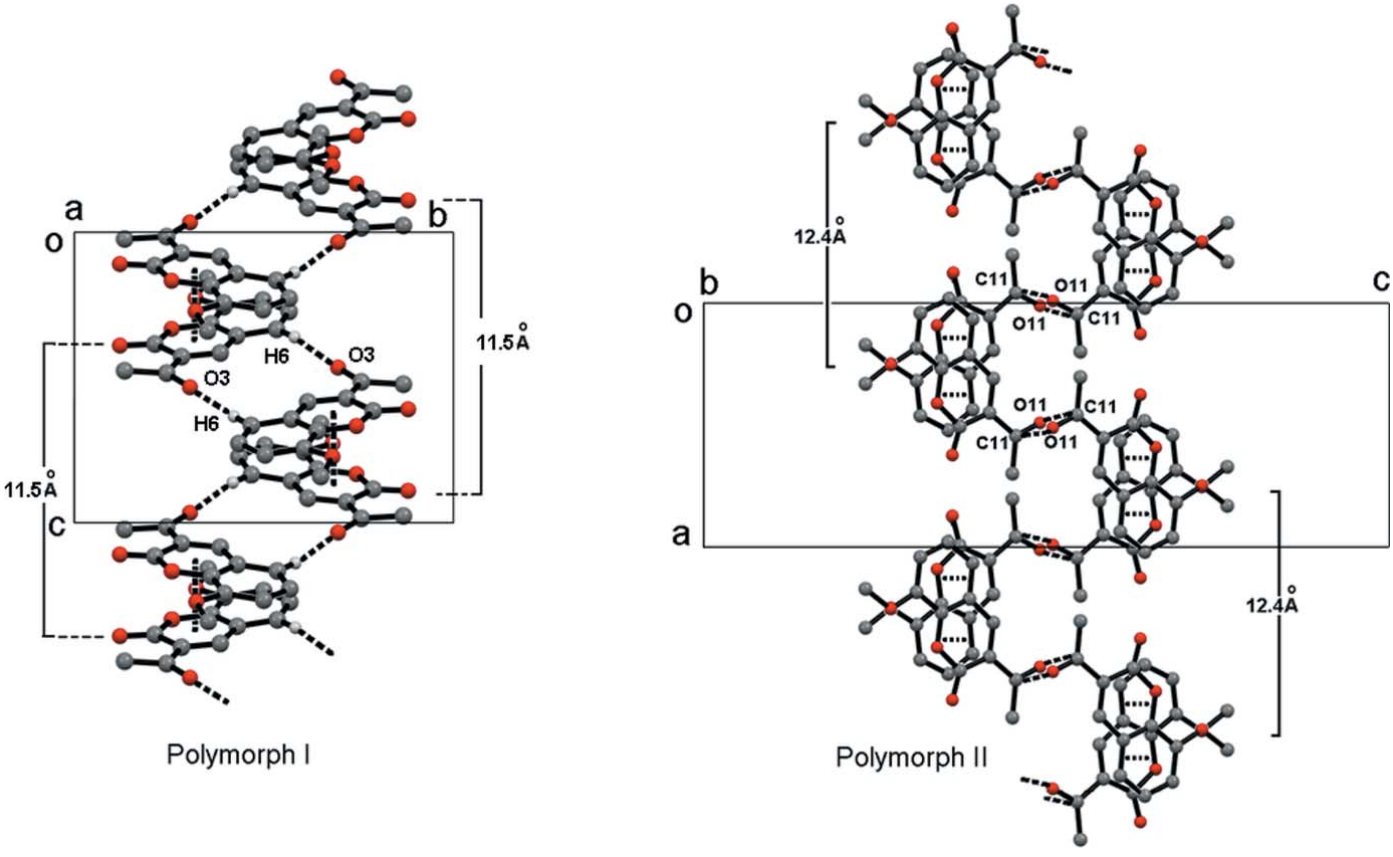

Figure 3
Helical conformation in the packing of polymorphs I and II of 3-acetyl-8-methoxy-2*H*-chromen-2-one. Dotted lines depict intermolecular interactions.

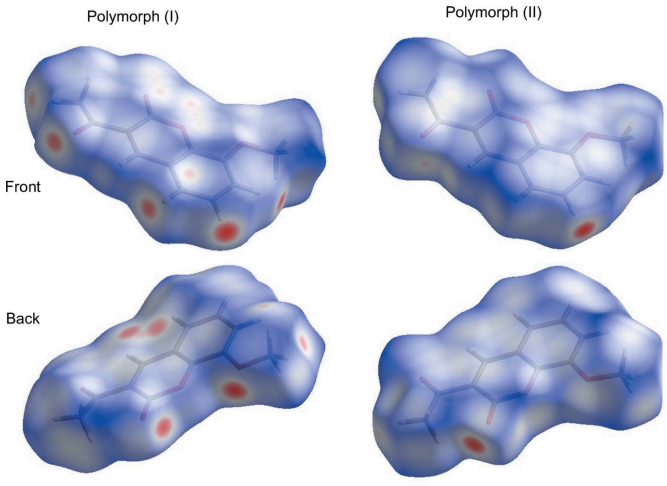

Figure 4
Hirshfeld surfaces for polymorphs I and II showing both sides of the molecules. Red areas represent contacts shorter than the sum of the van der Waals radii, blue areas represent zones where the shortest distance between atoms is larger than the sum of van der Waals radii and white areas are zones close to the sum of van der Waals radii.

forces in the crystal formation of both polymorphs are H···H and O···H interactions, but C···O and C···H short contacts in polymorph I make slightly bigger contributions to build the lattice, while in polymorph II, hydrogen bonding and π–π stacking contribute in greater proportions.

5. Database survey

A search of the Cambridge Structural Database (version 5.39, February 2018; Groom *et al.*, 2016) revealed only one crystal structure of the title compound (Refcode TEBFAJ; Li *et al.*, 2012). This structure, which we call polymorph I, is assembled by parallel flat sheets that extend along the *b* axis. It is worth mentioning that the acetyl coumarin without any substituent also forms at least two polymorphic forms (*A* and *B*; Munshi *et al.*, 2004) with subtle differences in intermolecular interactions, which include weak C—H···O and C—H··· π interactions. Form *A* crystallizes with head-to-head stacking being favored during nucleation, while form *B* prefers a head-to tail-stacking. This is similar to the two polymorphs of the title compound.

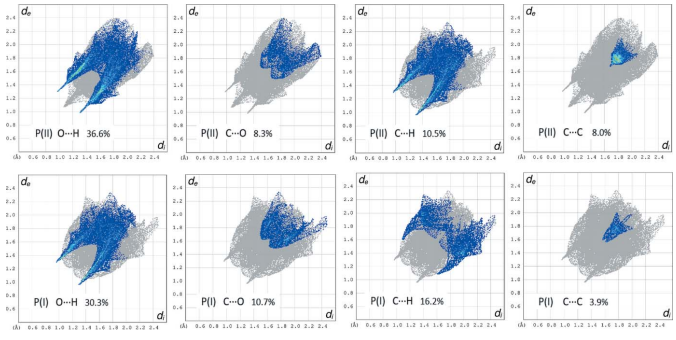

Figure 5
Comparison of several intermolecular interactions (blue areas) involved in the crystal packing of polymorphs I and II by decomposition of two-dimensional fingerprint plots. Green areas represent a greater abundance of close contacts and the full fingerprint appears beneath each decomposed plot as a grey shadow.

Table 2
Experimental details.

Crystal data	
Chemical formula	$C_{12}H_{10}O_4$
M_r	218.20
Crystal system, space group	Orthorhombic, *Pbca*
Temperature (K)	293
a, *b*, *c* (Å)	9.4973 (13), 7.9733 (11), 26.682 (4)
V (Å^3)	2020.5 (5)
Z	8
Radiation type	Mo *K*α
μ (mm^{-1})	0.11
Crystal size (mm)	0.40 × 0.35 × 0.30 × 0.15 (radius)
Data collection	
Diffractometer	Bruker APEXII area detector
Absorption correction	For a sphere [the interpolation procedure of Dwiggins (1975) was used with some modification]
T_{min}, T_{max}	0.861, 0.862
No. of measured, independent and observed [$I > 2\sigma(I)$] reflections	15317, 2453, 1798
R_{int}	0.045
(sin $\theta/\lambda)_{max}$ (Å^{-1})	0.667
Refinement	
$R[F^2 > 2\sigma(F^2)]$, $wR(F^2)$, *S*	0.041, 0.116, 1.10
No. of reflections	2453
No. of parameters	148
H-atom treatment	H-atom parameters constrained
$\Delta\rho_{max}$, $\Delta\rho_{min}$ (e Å^{-3})	0.20, −0.19

Computer programs: *APEX2* and *SAINT* (Bruker, 2004), *SHELXS97* and *SHELXL97* (Sheldrick, 2008), *SHELXL2018* (Sheldrick, 2015), *Mercury* (Macrae *et al.*, 2008), *WinGX2003* (Farrugia, 2012) and *PLATON* (Spek, 2009).

6. Synthesis and crystallization

The title compound was obtained *via* Knoevenagel condensation. 3-Methoxysalicylaldehyde and ethyl acetoacetate in a 1:1 molar ratio were loaded in a flask with ethyl alcohol as solvent and piperidine as catalyst and left under stirring and reflux for 5 h. The product was filtered and washed with cold ethanol followed by recrystallization from ethanol to yield the title compound as colourless crystals, 88% yield, mp 444–447 K; IR νKBr (cm^{-1}): 1727 (OC═O), 1682 (C═O), 1278, 1197 (C—O). NMR ^{1}H (δ ppm, $CDCl_3$): 8.42 (*s*, 1H, H-4); 7.25

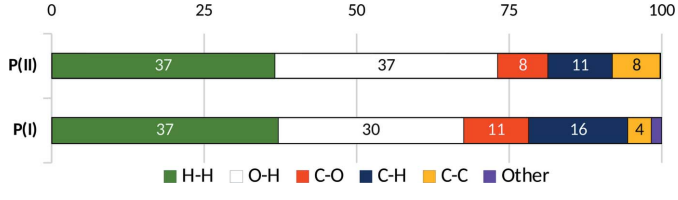

Figure 6
Relative contributions to the Hirshfeld surface for the major intermolecular contacts in polymorphs I and II.

(*d*, 1H, H-7, ^3J = 1.1, ^4J = 5.7 Hz), 7.18 (*t*, 1H, H-6, ^3J = 5.5, 2.0 Hz) 7.14 (*d*, 1H, H-5, ^3J = 2.0, ^4J = 5.7 Hz), 3.94 (*s*, 3H, OCH_3), 2.68 (*s*, 3H, H-12). NMR ^{13}C (δ ppm, $CDCl_3$): 195.8 (C-11), 158.9 (C-2), 147.9 (C-4), 147.2 (C-8), 145.1 (C-9), 125.0 (C-5), 124.8 (C-3), 121.5 (C-6), 118.9 (C-10), 116.0 (C-7), 56.5 (OCH_3), 30.8 (C-12). EA (%) calculated for $C_{12}H_{10}O_4$: 66.05 C, 4.62 H; found: 66.15 C, 4.60 H.

7. Refinement

Crystal data, data collection and structure refinement details are summarized in Table 2. H atoms were positioned geometrically and treated as riding atoms, with C—H = 0.93–0.98 Å and U_{iso}(H) = 1.2U_{eq}(C).

Acknowledgements

The authors thank Juan Pablo Mojica Sánchez for his contribution to the Hirshfeld surfaces calculation.

Funding information

GGC thanks CONACYT (Mexico) for PhD scholarship No. 364826.

References

Allen, F. H., Baalham, C. A., Lommerse, J. P. M. & Raithby, P. R. (1998). *Acta Cryst.* B**54**, 320–329.

Bruker (2004). *APEX2* and *SAINT*. Bruker AXS Inc., Madison, Wisconsin, USA.

Dwiggins, C. W. (1975). *Acta Cryst.* A**31**, 146–148.

Farrugia, L. J. (2012). *J. Appl. Cryst.* **45**, 849–854.

Gaudino, E. C., Tagliapietra, S., Martina, K., Palmisano, G. & Cravotto, G. (2016). *RSC Adv.* **6**, 46394–46405.

Gómez-Castro, C. Z., Padilla-Martínez, I. I., García-Báez, E. V., Castrejón-Flores, J. L., Peraza-Campos, A. L. & Martínez-Martínez, F. J. (2014). *Molecules*, **19**, 14446–14460.

González-Padilla, J. E., Rosales-Hernández, M. C., Padilla-Martínez, I. I., García-Báez, E. V., Rojas-Lima, S. & Salazar-Pereda, V. (2014). *Acta Cryst.* C**70**, 55–59.

Groom, C. R., Bruno, I. J., Lightfoot, M. P. & Ward, S. C. (2016). *Acta Cryst.* B**72**, 171–179.

Hasija, A. & Chopra, D. (2019). *Acta Cryst.* C**75**, 451–461.

Li, J., Li, X. & Wang, S. (2012). *Chin. J. Struct. Chem.* **31**, 1003–1007.

Liu, Y., Wang, Q. L., Zhou, C. S., Xiong, B. Q., Zhang, P. L., Kang, S. J., Yang, C. A. & Tang, K. W. (2018). *Tetrahedron Lett.* **59**, 2038–2041.

Macrae, C. F., Bruno, I. J., Chisholm, J. A., Edgington, P. R., McCabe, P., Pidcock, E., Rodriguez-Monge, L., Taylor, R., van de Streek, J. & Wood, P. A. (2008). *J. Appl. Cryst.* **41**, 466–470.

Munshi, P., Venugopala, K. N., Jayashree, B. S. & Guru Row, T. N. (2004). *Cryst. Growth Des.* **4**, 1105–1107.

Salem, M. A., Helal, M. H., Gouda, M. A., Ammar, Y. A., El-Gaby, M. S. A. & Abbas, S. Y. (2018). *Synth. Commun.* **48**, 1534–1550.

Santos-Contreras, R. J., Martínez-Martínez, F. J., Mancilla-Margalli, N. A., Peraza-Campos, A. L., Morín-Sánchez, L. M., García-Báez, E. V. & Padilla-Martínez, I. I. (2009). *CrystEngComm*, **11**, 1451–1461.

Sheldrick, G. M. (2008). *Acta Cryst.* A**64**, 112–122.

Sheldrick, G. M. (2015). *Acta Cryst*. C**71**, 3–8.

Spek, A. L. (2009). *Acta Cryst.* D**65**, 148–155.

Turner, M. J., McKinnon, J. J., Wolff, S. K., Grimwood, D. J., Spackman, P. R., Jayatilaka, D. & Spackman, M. A. (2017). *CrystalExplorer17. University of Western Australia.* http://hirshfeldsurface.net.

Vekariya, R. H. & Patel, H. D. (2014). *Synth. Commun.* **44**, 2756–2788.

supporting information

Acta Cryst. (2019). E**75**, 1866-1870 [https://doi.org/10.1107/S2056989019015159]

Crystal structure of a new polymorph of 3-acetyl-8-methoxy-2*H*-chromen-2-one

Gabino Gonzalez-Carrillo, Roberto Muñiz-Valencia, Efren V. García-Báez and Francisco J. Martínez-Martínez

Computing details

Data collection: *APEX2* (Bruker, 2004); cell refinement: *SAINT* (Bruker, 2004); data reduction: *SAINT* (Bruker, 2004); program(s) used to solve structure: *SHELXS97* (Sheldrick, 2008); program(s) used to refine structure: *SHELXL2018* (Sheldrick, 2015); molecular graphics: *Mercury* (Macrae *et al.*, 2008) and *WinGX2003* (Farrugia, 2012); software used to prepare material for publication: *SHELXL97* (Sheldrick, 2008), *WinGX2003* (Farrugia, 2012) and *PLATON* (Spek, 2009).

3-Acetyl-8-methoxy-2*H*-chromen-2-one

Crystal data

$C_{12}H_{10}O_4$
$M_r = 218.20$
Orthorhombic, *Pbca*
$a = 9.4973$ (13) Å
$b = 7.9733$ (11) Å
$c = 26.682$ (4) Å
$V = 2020.5$ (5) Å^3
$Z = 8$
$F(000) = 912$
$D_x = 1.435$ Mg m^{-3}
Mo $K\alpha$ radiation, $\lambda = 0.71073$ Å
Cell parameters from 600 reflections
$\theta = 20$–25°
$\mu = 0.11$ mm^{-1}
$T = 293$ K
Prism, colorless
0.40 × 0.35 × 0.30 × 0.15 (radius) mm

Data collection

Bruker APEXII area detector diffractometer
Radiation source: fine-focus sealed tube
Graphite monochromator
φ and ω scans
Absorption correction: for a sphere [the interpolation procedure of Dwiggins (1975) was used with some modification]
$T_{min} = 0.861$, $T_{max} = 0.862$
15317 measured reflections
2453 independent reflections
1798 reflections with $I > 2\sigma(I)$
$R_{int} = 0.045$
$\theta_{max} = 28.3°$, $\theta_{min} = 1.5°$
$h = -12 \rightarrow 12$
$k = -10 \rightarrow 10$
$l = -34 \rightarrow 35$

Refinement

Refinement on F^2
Least-squares matrix: full
$R[F^2 > 2\sigma(F^2)] = 0.041$
$wR(F^2) = 0.116$
$S = 1.10$
2453 reflections
148 parameters
0 restraints
Hydrogen site location: inferred from neighbouring sites
H-atom parameters constrained
$w = 1/[\sigma^2(F_o^2) + (0.0608P)^2 + 0.0858P]$ where $P = (F_o^2 + 2F_c^2)/3$
$(\Delta/\sigma)_{max} < 0.001$
$\Delta\rho_{max} = 0.20$ e Å^{-3}
$\Delta\rho_{min} = -0.19$ e Å^{-3}
Extinction correction: SHELXL2018 (Sheldrick, 2015), $Fc^* = kFc[1+0.001xFc^2\lambda^3/\sin(2\theta)]^{-1/4}$
Extinction coefficient: 0.0117 (15)

Special details

Geometry. All esds (except the esd in the dihedral angle between two l.s. planes) are estimated using the full covariance matrix. The cell esds are taken into account individually in the estimation of esds in distances, angles and torsion angles; correlations between esds in cell parameters are only used when they are defined by crystal symmetry. An approximate (isotropic) treatment of cell esds is used for estimating esds involving l.s. planes.

Fractional atomic coordinates and isotropic or equivalent isotropic displacement parameters (Å²)

	x	*y*	*z*	U_{iso}*/U_{eq}
C2	0.50500 (12)	0.47624 (16)	0.37371 (4)	0.0424 (3)
C3	0.44835 (12)	0.56358 (15)	0.41705 (4)	0.0382 (3)
C4	0.30805 (13)	0.57565 (15)	0.42255 (4)	0.0410 (3)
H4	0.272844	0.632762	0.450238	0.049*
C5	0.06405 (13)	0.51543 (17)	0.39234 (5)	0.0503 (3)
H5	0.023660	0.571130	0.419379	0.060*
C6	−0.01876 (14)	0.44331 (19)	0.35668 (6)	0.0561 (4)
H6	−0.116156	0.450497	0.359563	0.067*
C7	0.03947 (14)	0.35925 (18)	0.31610 (5)	0.0512 (4)
H7	−0.019498	0.311173	0.292263	0.061*
C8	0.18326 (13)	0.34597 (15)	0.31060 (4)	0.0410 (3)
C9	0.26746 (12)	0.42080 (14)	0.34702 (4)	0.0364 (3)
C10	0.21098 (12)	0.50478 (14)	0.38783 (4)	0.0389 (3)
C11	0.54296 (14)	0.64209 (16)	0.45541 (4)	0.0457 (3)
C12	0.69794 (15)	0.6292 (2)	0.45047 (6)	0.0645 (4)
H12A	0.724728	0.513243	0.449103	0.097*
H12B	0.742035	0.681599	0.478819	0.097*
H12C	0.727490	0.684582	0.420301	0.097*
C14	0.17018 (17)	0.1828 (2)	0.23613 (5)	0.0637 (4)
H14A	0.111460	0.262506	0.219101	0.096*
H14B	0.112261	0.099779	0.252075	0.096*
H14C	0.231370	0.129280	0.212366	0.096*
O1	0.40976 (8)	0.40859 (11)	0.34056 (3)	0.0415 (2)
O2	0.62587 (9)	0.45659 (16)	0.36291 (4)	0.0728 (4)
O11	0.49013 (11)	0.71394 (14)	0.49062 (4)	0.0688 (3)
O13	0.25265 (9)	0.26717 (11)	0.27307 (3)	0.0524 (3)

Atomic displacement parameters (Å²)

	U^{11}	U^{22}	U^{33}	U^{12}	U^{13}	U^{23}
C2	0.0323 (6)	0.0528 (8)	0.0422 (6)	−0.0022 (5)	−0.0010 (5)	−0.0078 (5)
C3	0.0384 (6)	0.0398 (7)	0.0366 (6)	−0.0002 (5)	0.0004 (5)	−0.0005 (5)
C4	0.0432 (7)	0.0407 (7)	0.0391 (6)	0.0040 (5)	0.0075 (5)	0.0005 (5)
C5	0.0355 (7)	0.0548 (8)	0.0608 (8)	0.0073 (6)	0.0079 (6)	0.0094 (6)
C6	0.0287 (6)	0.0638 (9)	0.0756 (9)	0.0034 (6)	−0.0017 (6)	0.0203 (8)
C7	0.0383 (7)	0.0542 (8)	0.0612 (8)	−0.0070 (6)	−0.0140 (6)	0.0146 (7)
C8	0.0377 (7)	0.0424 (7)	0.0428 (6)	−0.0039 (5)	−0.0060 (5)	0.0087 (5)
C9	0.0290 (6)	0.0389 (6)	0.0413 (6)	−0.0007 (5)	−0.0014 (4)	0.0072 (5)
C10	0.0341 (6)	0.0387 (7)	0.0439 (6)	0.0031 (5)	0.0041 (5)	0.0075 (5)

C11	0.0530 (8)	0.0441 (7)	0.0400 (6)	−0.0015 (6)	−0.0030 (5)	−0.0030 (5)
C12	0.0495 (8)	0.0822 (11)	0.0619 (8)	−0.0103 (7)	−0.0129 (7)	−0.0193 (8)
C14	0.0738 (10)	0.0702 (10)	0.0472 (8)	−0.0148 (8)	−0.0223 (7)	−0.0020 (7)
O1	0.0292 (4)	0.0548 (5)	0.0406 (4)	−0.0015 (4)	−0.0003 (3)	−0.0094 (4)
O2	0.0288 (5)	0.1185 (10)	0.0710 (7)	−0.0005 (5)	0.0019 (4)	−0.0424 (7)
O11	0.0716 (7)	0.0821 (8)	0.0527 (6)	0.0059 (6)	−0.0036 (5)	−0.0262 (5)
O13	0.0503 (6)	0.0613 (6)	0.0455 (5)	−0.0085 (4)	−0.0092 (4)	−0.0084 (4)

Geometric parameters (Å, º)

C2—O2	1.1940 (14)	C8—O13	1.3535 (15)
C2—O1	1.3753 (14)	C8—C9	1.3929 (16)
C2—C3	1.4530 (16)	C9—O1	1.3659 (14)
C3—C4	1.3440 (16)	C9—C10	1.3863 (16)
C3—C11	1.4991 (17)	C11—O11	1.2094 (15)
C4—C10	1.4238 (17)	C11—C12	1.481 (2)
C4—H4	0.9300	C12—H12A	0.9600
C5—C6	1.362 (2)	C12—H12B	0.9600
C5—C10	1.4032 (17)	C12—H12C	0.9600
C5—H5	0.9300	C14—O13	1.4275 (15)
C6—C7	1.388 (2)	C14—H14A	0.9600
C6—H6	0.9300	C14—H14B	0.9600
C7—C8	1.3776 (17)	C14—H14C	0.9600
C7—H7	0.9300		
O2—C2—O1	115.19 (11)	O1—C9—C8	116.70 (10)
O2—C2—C3	127.66 (11)	C10—C9—C8	122.20 (11)
O1—C2—C3	117.15 (10)	C9—C10—C5	118.77 (11)
C4—C3—C2	119.23 (10)	C9—C10—C4	116.89 (11)
C4—C3—C11	119.32 (11)	C5—C10—C4	124.34 (11)
C2—C3—C11	121.44 (10)	O11—C11—C12	120.94 (12)
C3—C4—C10	122.85 (11)	O11—C11—C3	118.66 (12)
C3—C4—H4	118.6	C12—C11—C3	120.40 (11)
C10—C4—H4	118.6	C11—C12—H12A	109.5
C6—C5—C10	119.27 (13)	C11—C12—H12B	109.5
C6—C5—H5	120.4	H12A—C12—H12B	109.5
C10—C5—H5	120.4	C11—C12—H12C	109.5
C5—C6—C7	121.25 (12)	H12A—C12—H12C	109.5
C5—C6—H6	119.4	H12B—C12—H12C	109.5
C7—C6—H6	119.4	O13—C14—H14A	109.5
C8—C7—C6	121.00 (12)	O13—C14—H14B	109.5
C8—C7—H7	119.5	H14A—C14—H14B	109.5
C6—C7—H7	119.5	O13—C14—H14C	109.5
O13—C8—C7	126.67 (11)	H14A—C14—H14C	109.5
O13—C8—C9	115.82 (11)	H14B—C14—H14C	109.5
C7—C8—C9	117.51 (12)	C9—O1—C2	122.79 (9)
O1—C9—C10	121.09 (10)	C8—O13—C14	117.55 (11)

O2—C2—C3—C4	178.80 (14)	O1—C9—C10—C4	−0.53 (16)
O1—C2—C3—C4	−0.59 (17)	C8—C9—C10—C4	179.87 (11)
O2—C2—C3—C11	−0.5 (2)	C6—C5—C10—C9	0.02 (18)
O1—C2—C3—C11	−179.90 (10)	C6—C5—C10—C4	179.73 (12)
C2—C3—C4—C10	0.63 (18)	C3—C4—C10—C9	−0.08 (17)
C11—C3—C4—C10	179.96 (11)	C3—C4—C10—C5	−179.79 (11)
C10—C5—C6—C7	0.2 (2)	C4—C3—C11—O11	0.34 (18)
C5—C6—C7—C8	0.0 (2)	C2—C3—C11—O11	179.66 (12)
C6—C7—C8—O13	179.70 (11)	C4—C3—C11—C12	179.43 (12)
C6—C7—C8—C9	−0.40 (18)	C2—C3—C11—C12	−1.25 (18)
O13—C8—C9—O1	0.88 (15)	C10—C9—O1—C2	0.57 (16)
C7—C8—C9—O1	−179.03 (10)	C8—C9—O1—C2	−179.80 (11)
O13—C8—C9—C10	−179.50 (10)	O2—C2—O1—C9	−179.47 (12)
C7—C8—C9—C10	0.58 (17)	C3—C2—O1—C9	0.00 (16)
O1—C9—C10—C5	179.20 (10)	C7—C8—O13—C14	−2.70 (18)
C8—C9—C10—C5	−0.40 (17)	C9—C8—O13—C14	177.40 (11)

Hydrogen-bond geometry (Å, º)

D—H···*A*	*D*—H	H···*A*	*D*···*A*	*D*—H···*A*
C12—H12*B*···O11^{i}	0.96	2.63	3.4255 (17)	141
C6—H6···O2^{ii}	0.93	2.45	3.3808 (16)	176
C14—H14*A*···O2^{iii}	0.96	2.68	3.4535 (18)	138
C4—H4···O11	0.93	2.42	2.7395 (16)	100
C12—H12*A*···O2	0.96	2.52	2.797 (2)	97

Symmetry codes: (i) *x*+1/2, −*y*+3/2, −*z*+1; (ii) *x*−1, *y*, *z*; (iii) *x*−1/2, *y*, −*z*+1/2.